Jordan Journal of Energy
Volume 1, Number 2, 2023

ISSN (Online): 2790-7678
ISSN (Print): 2790-766X

Jordan Journal of Energy (JJE)
Journal Homepage: http://dsr.mutah.edu.jo/index.php/jje
JEE an official peer review journal of Mutah University,

Damping Undammed Low Frequency Oscillations in Power Systems: An ANN-Based Approach Using Pre-Disturbance Data

Mohammad M. Al-Momani[1]*, Amneh Al-Mbaideen[2], Seba F. Al-Gharaibeh[2],

*[1]Electrical Engineering department, Iowa State University, Ames, USA

mmomani@iastate.edu

[2]Mutah University, Electrical Engineering Department, Jordan

a.mbaideen@mutah.edu.jo

Received 14th June 2023; Accepted 12th August 2023

*Corresponding Author Email: mmomani@iastate.edu, monqedmohammad@gmail.com

ABSTRACT. *The paper examines undammed low frequency oscillations (LFOs) that can lead to system collapse, citing the Jordan power network incident on May 21, 2021. Traditional model-based methods for studying LFOs' small-signal stability have limitations. To address this, an online damping controller based on an artificial neural network (ANN) is proposed. Unlike existing ANN-based methods relying on offline controllers, this novel approach utilizes pre-disturbance data from phasor measurement units (PMUs) to dampen oscillations effectively. The paper addresses challenges of partially observable systems in online eigenvalue prediction using ANN. MATLAB is used to implement a feedforward ANN system trained on PMU data. The study involves a three-area test system with various operational scenarios, training the ANN across 406 scenarios to predict eigenvalues and damp LFOs.*

Keywords: Undammed low frequency oscillations (LFOs), System collapse, Small-signal stability, Model-based methods, Measurement-based identification, Phasor measurement units (PMUs), Wide area damping controller, artificial neural network (ANN), Post-disturbance data, Ring-down method.

1. Introduction. The paper presented herein delves into the critical analysis of undammed low frequency oscillations (LFOs) and their potential repercussions, notably demonstrated by the incident in the Jordan power network on May 21, 2021. These oscillations, with the capacity to induce system collapse, are intricately linked to small-signal stability in power networks. Traditional approaches for understanding LFOs, primarily reliant on model-based techniques, have shown limitations as expounded in prior research. In response, this paper introduces an innovative solution in the form of an online wide area damping controller. This controller is grounded in artificial neural network (ANN) technology and is adept at identifying LFOs through real-time data acquired from phasor measurement units (PMUs). Unlike prevailing

methods, which necessitate offline controllers, the proposed approach leverages pre-disturbance data, eliminating the need for such controllers. The paper also addresses the challenges posed by partial observability in predicting system behavior using ANN. The study emulates real-world scenarios, particularly focusing on the Jordanian power system, while incorporating fully observable systems as a representation of the future landscape. Employing a feedforward ANN system with a backpropagation training algorithm implemented in MATLAB, the research utilizes comprehensive PMU measurements encompassing generator angles, reactive powers, and bus angles. Through an extensive array of operational scenarios, the paper trains the ANN to predict eigenvalues, providing a robust framework for effectively managing and mitigating the impact of LFOs in power networks.

The utilization of advanced wide-area monitoring through the incorporation of phasor measurement units (PMUs) facilitates a continuous evaluation of the operational health of power grid systems. Over the past two decades, the practice of dynamically monitoring power systems for real-time operation and control has become increasingly prominent within the field. A spectrum of both linear and nonlinear methodologies have been proposed by scholars to effectively gauge the dynamic responses and proficiently estimate the key parameters associated with prevailing low-frequency oscillatory modes. The assessment of power system modes is conventionally carried out through two distinct avenues: the modal-based approach, characterized by its propensity to linearize governing equations surrounding operational points [1], and the measurement-based approach, which inherently engages in data-driven analyses of system measurement data [2]. The IEEE task force focused on the identification of electromechanical oscillatory modes substantiates a comprehensive compendium of techniques deployed across modal and data-driven paradigms [3]. Although the efficacy of model-based techniques in accommodating the intricacies of large-scale power systems is restricted due to computational exigencies, concurrently, measurement-based methods, particularly those harnessing synchrophasor technology, are widely adopted to discern and delineate low-frequency modes [4]. This category of measurement-based techniques, encompassing methodologies such as Prony analysis [5], matrix pencil method (MPM) [6], signal parameter estimation via rotational invariant techniques (ESPRIT) [7], auto-regressive moving average (ARMA) technique [8], and eigenvalue realization algorithm (ERA) [9], is ubiquitously present within a myriad of scholarly works. These techniques feature prominently in investigations pertaining to ring-down oscillation studies. Similarly, concerning ambient oscillation studies, techniques encompass transfer function methods [10] alongside subspace methods [11], [12]. Notably, the subspace approach garners enhanced precision, thereby rendering superior results in terms of accuracy; nevertheless, transfer function methods persist as the favored recourse in consideration of computational efficiency [13].

This paper initiates by performing online mode identification through an Artificial Neural Network (ANN). Subsequently, the influence of partial observability on predicting online eigenvalues is addressed. The research employs a feedforward ANN system along with a

backpropagation training algorithm, executed using MATLAB 2020b. Each training dataset is partitioned into 80% for training, 10% for validation, and 10% for testing purposes. To validate the model, diverse scenarios are generated for each system after undergoing training within the MATLAB toolbox.

2. ANN-Based Electromechanical Modes Identification. Within this section, the estimation of electromechanical modes in the three-area test system with string configuration [14] is undertaken employing three distinct inputs: generators' angles, generators' reactive powers, and bus angles. These data sets can be effectively acquired using PMUs during the pre-fault duration.

The three-area test system [14] encompasses five PV synchronous generators and a slack generator. The angles of these generators are contingent upon the operational state and system topologies. Herein, an Artificial Neural Network (ANN) structure is trained utilizing generator angles across various scenarios. The ANN system is trained using a comprehensive set of 406 scenarios, comprising:

- Load 9 ranging from 1300 MW to 1900 MW, incremented by 100 MW, for operation point A.
- Load 12 ranging from 900 MW to 1500 MW, incremented by 100 MW, for operation point A.
- Load 16 ranging from 800 MW to 1500 MW, incremented by 100 MW, for operation point A.
- Load 12 ranging from 1300 MW to 1900 MW, incremented by 100 MW, for operation point B.
- Load 16 ranging from 900 MW to 1500 MW, incremented by 100 MW, for operation point B.
- Load 9 ranging from 800 MW to 1500 MW, incremented by 100 MW, for operation point B.
- Load 16 ranging from 1300 MW to 1900 MW, incremented by 100 MW, for operation point C.
- Load 9 ranging from 900 MW to 1500 MW, incremented by 100 MW, for operation point C.
- Load 12 ranging from 800 MW to 1500 MW, incremented by 100 MW, for operation point C.

All the aforementioned 63 scenarios are systematically replicated for various system topologies.

TABLE 1. Number of cases collected at different topologies.

Topology	Numbers of cases
Normal	63
TL9-16 tripped	63
TL12-16 tripped	63
TL15-16 tripped	63
TL9-16 and TL 15-16 are tripped	63
TL12-16 and TL 15-16 are tripped	63
TL9-16 and TL 12-16 are tripped	63
TL9-16, TL 12-16, and TL15-16 are tripped	63
Unsuccess Load flow	98
Total	406

An additional set of 160 validation cases has been meticulously selected to thoroughly scrutinize the proposed framework. These validation instances encompass a diverse range of load and capacitor values, introducing a comprehensive spectrum of scenarios.

Within each scenario, employing small-signal analysis (as elaborated [14]), the real and imaginary components of the eigenvalues (both local and interarea) are meticulously computed. The prediction of these five eigenvalues (comprising three local and two interarea modes) is executed through the utilization of four distinctive parameters:

- Generators' angles.
- Generators' reactive power.
- Generators and load voltage angles.
- Buses' voltage angles.

The configuration of each system engenders ten outputs, split into the real components (five outputs) and imaginary components (five outputs) of the eigenvalues. Every system undergoes five rounds of training, encompassing an exhaustive array of 100,000 diverse architectures, each characterized by varying numbers of layers and neurons. This encompasses all possible permutations of 1-5 layers housing 4-13 neurons per layer for each respective system. The outcome of this extensive experimentation is the identification of optimal structures that yield minimal mean square error for each system, as meticulously tabulated in Table 2.

TABLE 2. Optimal structures of the proposed ANN.

System input	No. Layer	No. Neurons per Layer
Generator buses' angles	4	[10 6 7 10]
Generators' reactive power	4	[10 10 11 11]
Buses' voltage angels	4	[7 11 9 11]
Generators and load buses' angles	4	[11 8 10 11]

The optimal structure for each system is trained 500 times. The optimal design is selected based on the mean square error of all 406 samples. The best mean square error of the training, validation, and testing stages are shown in Figures 1 to 4 for each system.

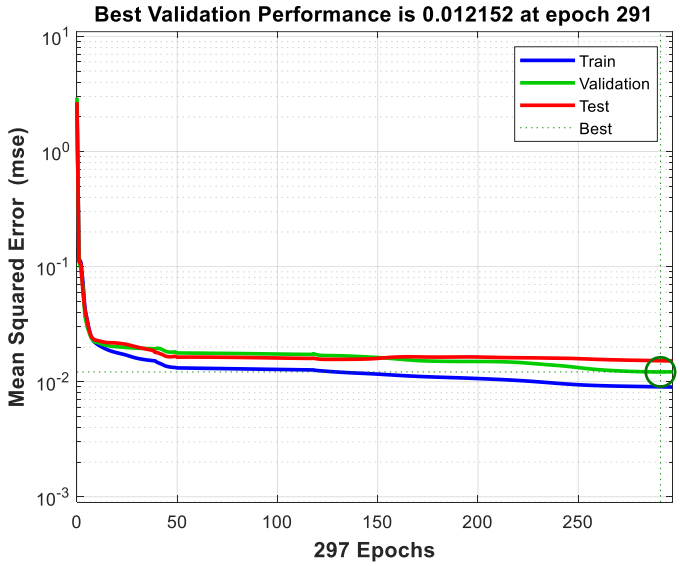

FIGURE 1. Performance criterion for the generator bus angle-based system.

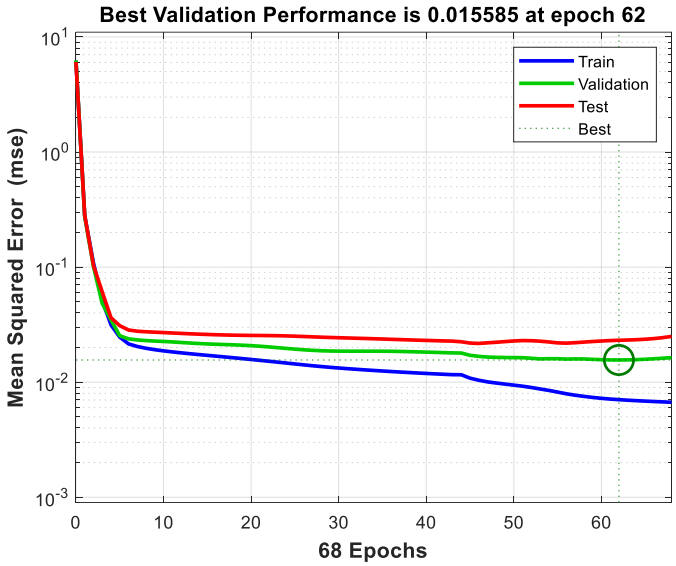

FIGURE 2. Performance criterion for the generator reactive power-based system.

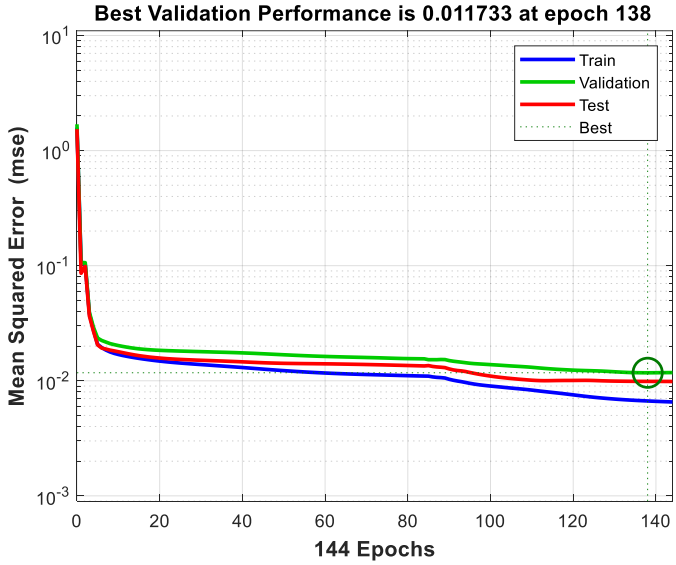

FIGURE 3. Performance criterion for the buses' angles-based system.

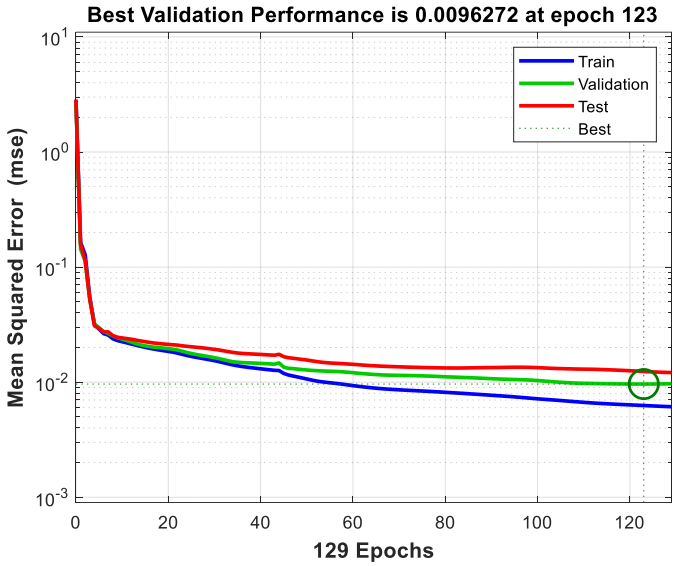

FIGURE 4. Performance criterion for generator and load bus angle-based system.

Figures 1 to 4 provide a comprehensive insight into the optimization process for each system's optimal structure, which was subjected to 500 training iterations. The selection of the most effective design was based on the mean square error calculated across all 406 samples. These figures elucidate the best mean square errors achieved throughout the training, validation, and testing stages for each individual system.

- Figure 1 illustrates the performance criterion for the system centered on generator bus angles. Notably, the graph showcases the evolution of validation performance, with the most noteworthy achievement being a validation performance of 0.012152, attained at epoch 291.
- Figure 2 outlines the performance criterion associated with the generator reactive power-based system. The graph captures the trajectory of validation performance over iterations, with the optimal validation performance of 0.015585 materializing at epoch 62.
- Figure 3 expounds upon the performance criterion for the bus angle-based system. The graph elegantly captures the fluctuations in validation performance, with a strikingly favourable validation performance of 0.011733 recorded at epoch 138.
- Figure 4 delineates the performance criterion for the system predicated on both generator and load bus angles. The graph showcases the dynamics of validation performance, culminating in a remarkable validation performance of 0.0096272, observed at epoch 123.

In essence, these figures meticulously portray the dynamic nature of the optimization process for each system's optimal structure, spotlighting the epochs at which the most favorable validation performances were achieved across the training iterations.

Based on the performance criterion depicted in Figure 4, the most optimal system is determined to be founded on generator and load bus angles. This particular system was refined over 123 iterations through the utilization of the backpropagation technique for training the ANN structure. The ensuing model is explored in the subsequent analysis.

The interconnections between layers, as showcased in Figure 5, contribute to elucidating the system's architecture. Within these figures, the larger squares represent relatively substantial values, while the smaller squares denote diminutive values. Moreover, the coloring of these

squares is indicative of the value's sign (negative: red (dark), positive: green (light)). These figures collectively grant insights into the relative magnitudes of the weights employed within the system.

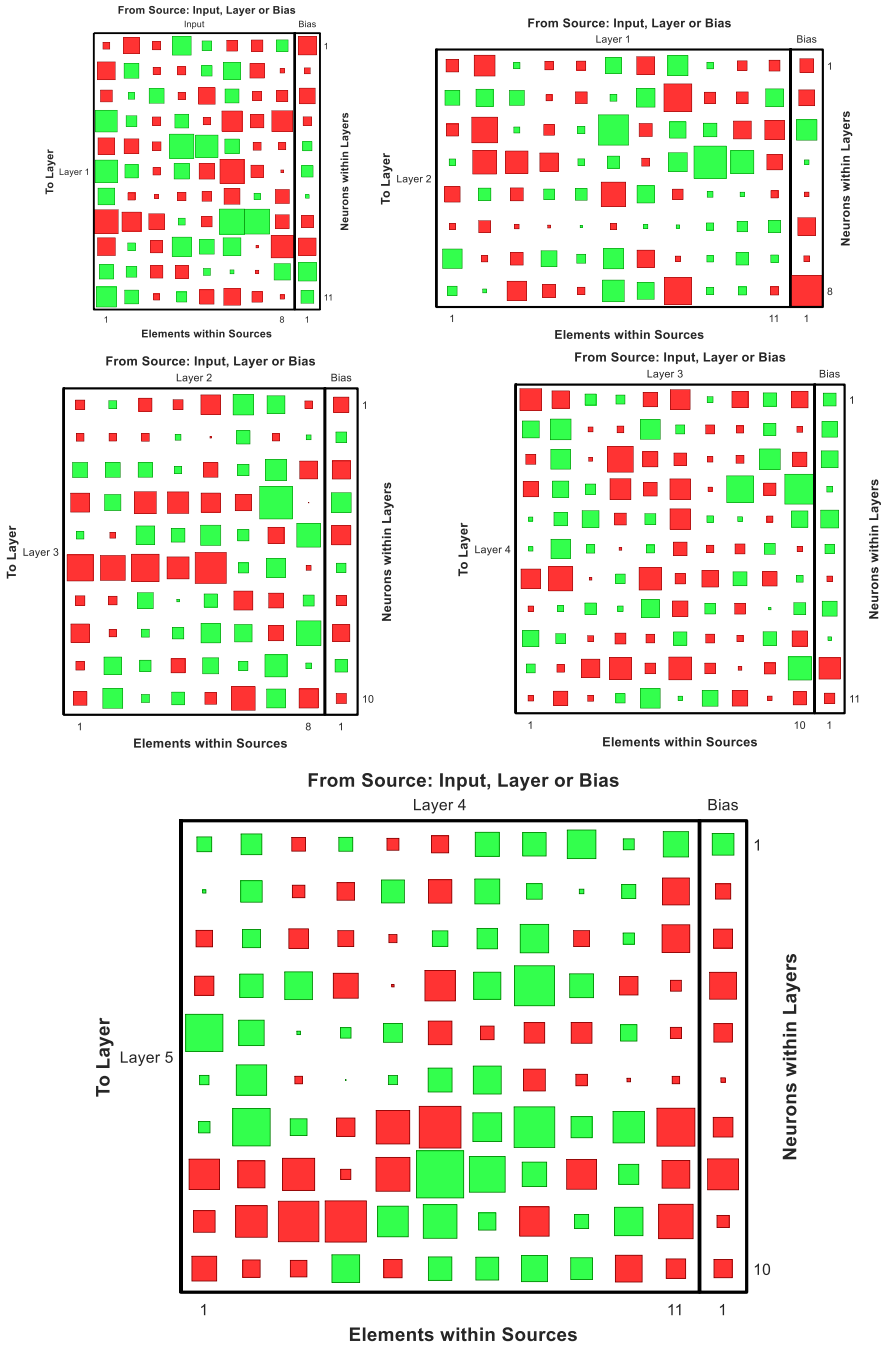

FIGURE 5. system Wights.

Figure 6 showcases the confusion matrix encompassing both interarea and local-area modes. This matrix serves to validate the efficacy of eigenvalue classification. As evident from Figure 6 (a), the accuracy of correct predictions stands at 98.3%, with a mere 1.7% attributed to incorrect predictions. The most pronounced confusion within outputs materializes between the initial two outputs, corresponding to the real parts of interarea eigenvalues. This occurrence is

deemed acceptable, given the proximity of real parts for both interarea modes. The concept underpinning the confusion matrix relies on a strict equality criterion with minimal tolerance. The robustness of the model is substantiated by the higher occurrence of correct predictions compared to incorrect ones. Consequentially, in light of these confusion matrix findings, the utilization of the mode index [15] is deemed unnecessary for oscillation mode categorization within this model.

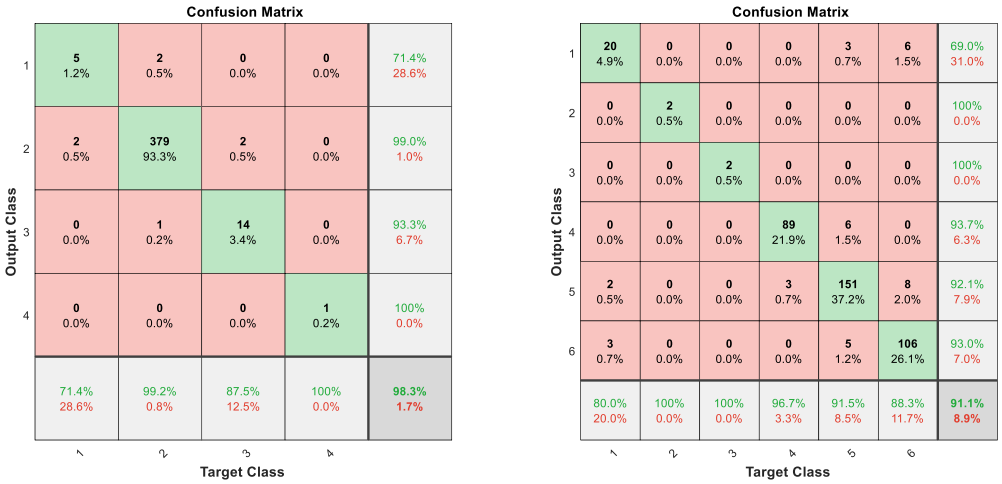

(a) (b)

FIGURE 6. Confusion matrix for (a) interarea modes (real 1, real 2, imaginary 1, imaginary 2) (b) local modes (real 1, real 2, real 3, imaginary 1, imaginary 2, imaginary 3)

The histogram error is presented in Figure 7. From Figure 7, the maximum error is within 0.002952. The online wide-area controller sensitivity should cover this error in both real and imaginary parts of the eigenvalues.

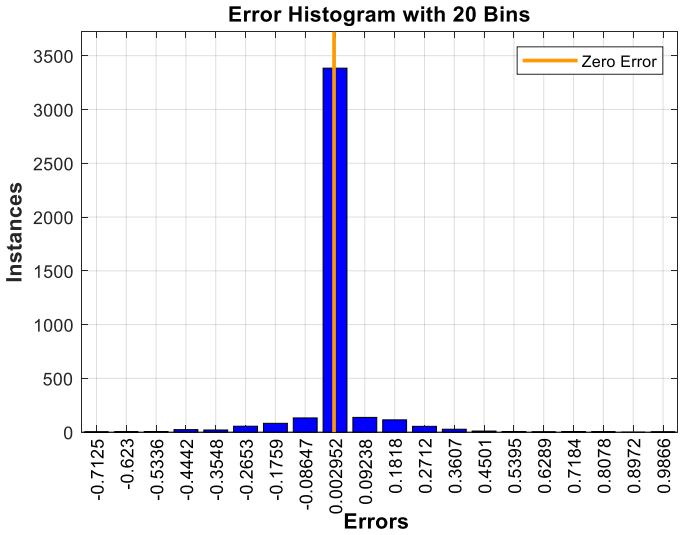

FIGURE 7. Histogram error for all samples (training samples)

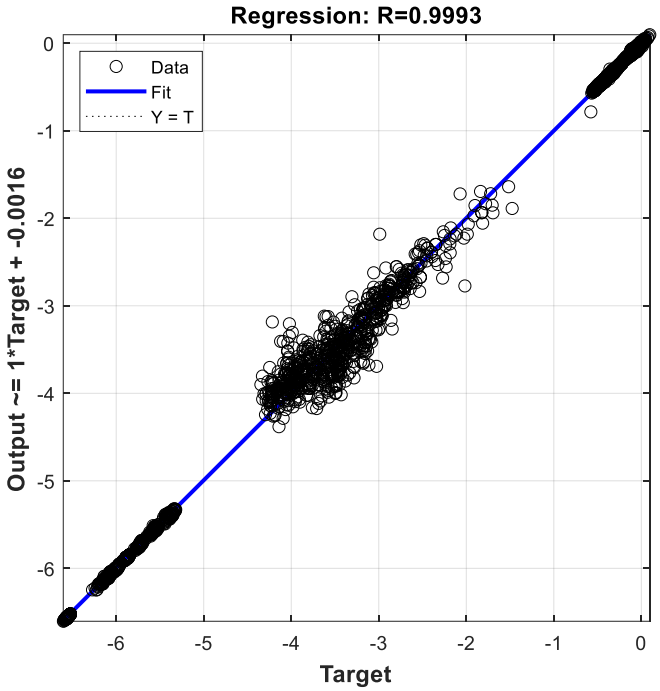

FIGURE 8. Output/target regression

Output and target regression for the trained data is presented in Figure 8. From the Figure, the behavior of the system is very good. The validation data (160 samples) is applied to the model, and the prediction eigenvalues and the true eigenvalues are plotted at the same graphs in Figures 9 for the local modes and Figure 10 for the interarea modes.

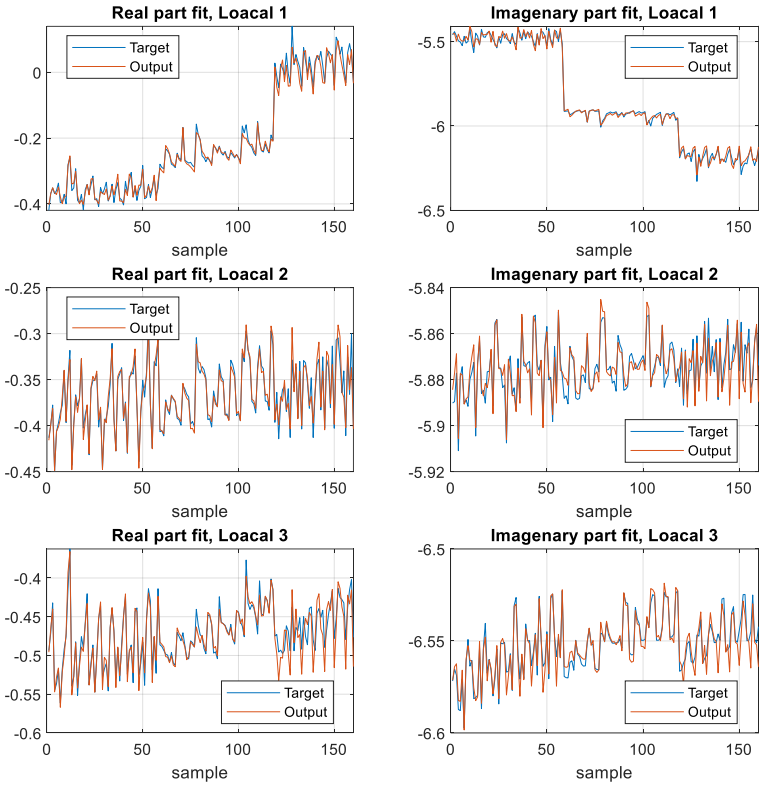

FIGURE **9.** Local modes prediction for the validation data (160 samples)

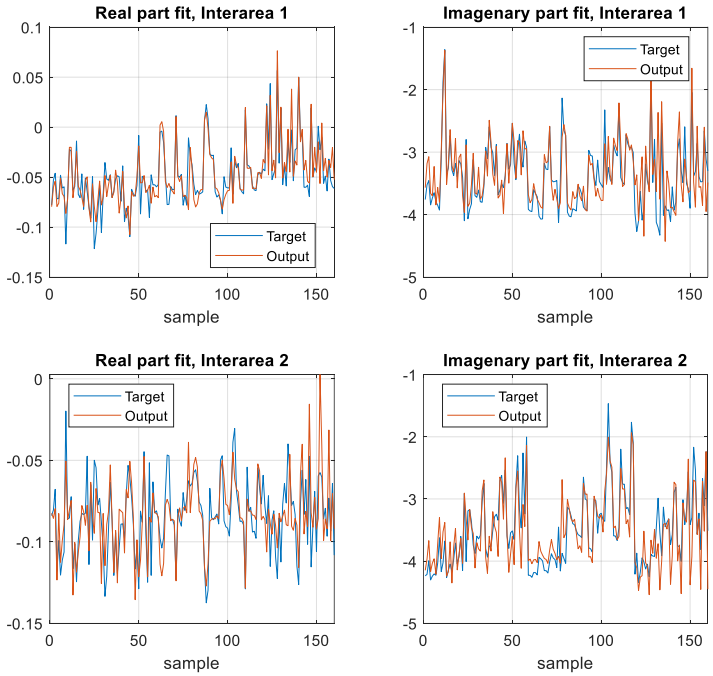

FIGURE **10**. Interarea modes prediction for the validation data (160 samples)

Figures 9 and 10 prove the effectiveness of the application of the ANN in eigenvalues' prediction using loads and generators angles. The fitting in the local-area modes is more accurate than that in the interarea modes.

3. Oscillation mode identification for partially observable system. In this section, the assumption that the first area's PMUs has a variance of (10^{-12}), the second area's PMUs has a variance of (10^{-11}) and the variance of the third area's PMUs is (10^{-10}). It supposed that the data of the SCADA system has a variance of (10^{-6}). Based on these assumptions, the measured data of each PMUs and the SCADA system are generated for all training (406 samples) and validation data (160 samples) in the previous section.

Based on [16], the optimal PMU placement for the partially observable system by PMUs is obtained (bus 4 then 11 then 14). The three scenarios are considered here to obtain the eigenvalues from the measured data. The trained generator and load angle model in the previous section is selected here

3.1. Partial Observable System by 1 PMU. In the three-area test system, three PMUs are needed to make the system fully observable. If the system is observable by the SCADA only, the white standard error with variance 10^{-6} are added to the actual data.

For the first PMU location (bus 4 or 11 or 14), the error from PMUs is added to the measured data. the eigenvalues (real and imaginary parts) of the five modes are estimated using the trained model in the previous section. The error between the actual outputs (real and imaginary part of the eigenvalues) and the estimated are:

Table 3. One PMU in the three-area test system.

Error	True data	SCADA data	One PMU at Bus 4	One PMU at Bus 11	One PMU at Bus 14
Average absolute	0.066398	0.068022	0.066511	0.067927	0.067981
Mean square	0.009904	0.010329	0.009943	0.010299	0.010321

From the table, the optimal location of the first PMU is bus 4. The average absolute error is decreased from 0.068022 to 0.066511 by the first PMU. For all locations (Bus 4, bus 11, or bus 14), the PMU enhances the prediction of the Eigenvalues. On the other hand, the high sampling rate of the PMUs makes the prediction is effective for the transient scenarios. The mean square error is also decreased for any location, but the optimal location (minimum error) is bus 4. The results validate the OPP for partial observability-based on the participation factor of the gain matrix.

Figure 11 shows the average absolute error of the 556 samples for different PMU location. From the figure, the real part of the first local mode (output 1) and the real part of the interarea modes (outputs 4 and 5) prediction are enhanced when a PMU is installed at bus 4. The imaginary part of the interarea mode 1 prediction is also enhanced (output 9). The absolute error in output 7 (imaginary part of the third local mode) is decreased in the case of the PMU installed at bus 4, but this output is not affected if the PMU is installed at other locations.

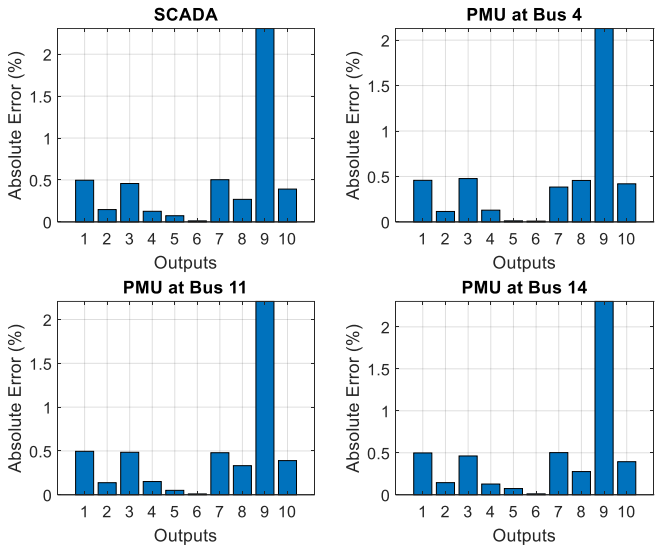

FIGURE **11**. Prediction eigenvalues error for the first PMU location

3.2. **Partial Observability System by 2 PMUs.** The first PMU is installed at bus 4. Two choices for the second PMU are available (buses 11 and 14). The average absolute error of each output prediction in these two choices is shown in figure 12. The average absolute error, and the mean square error of these locations are:

Table 4. Two PMUs in the three-area test system

Error	True data	SCADA data	PMUs at Bus 4 and 11	PMUs at Bus 4 and 14
Average absolute	0.066398	0.068022	0.066414	0.066486
Mean square	0.009904	0.010329	0.009911	0.009935

From the table, the optimal location of the second PMU is Bus 11. Once the third PMU is installed at bus 14, the average and mean square errors decrease to 0.066398, and 0.0009904, respectively. The results of the full system observability by PMUs are very close to the prediction using the true data. Figure 13 shows the average absolute error in case of the three PMUs are installed in the system (Full observable system).

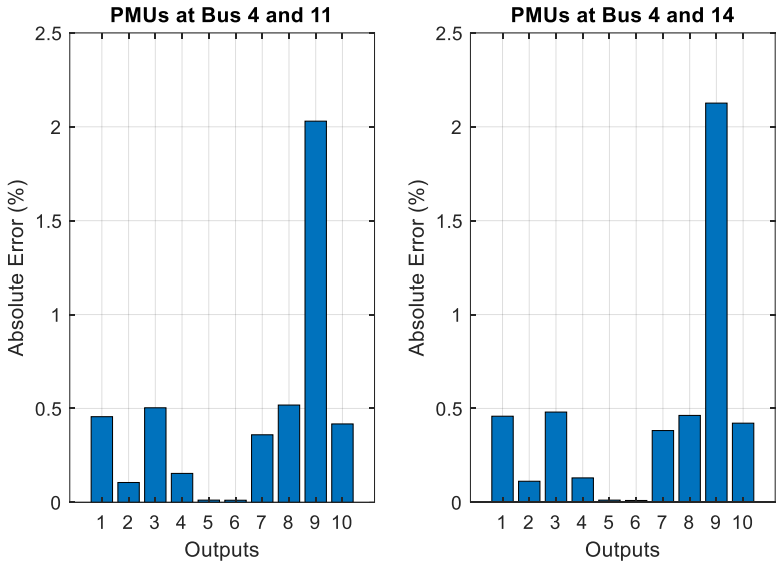

Figure 12. Prediction eigenvalues error for the second PMU location

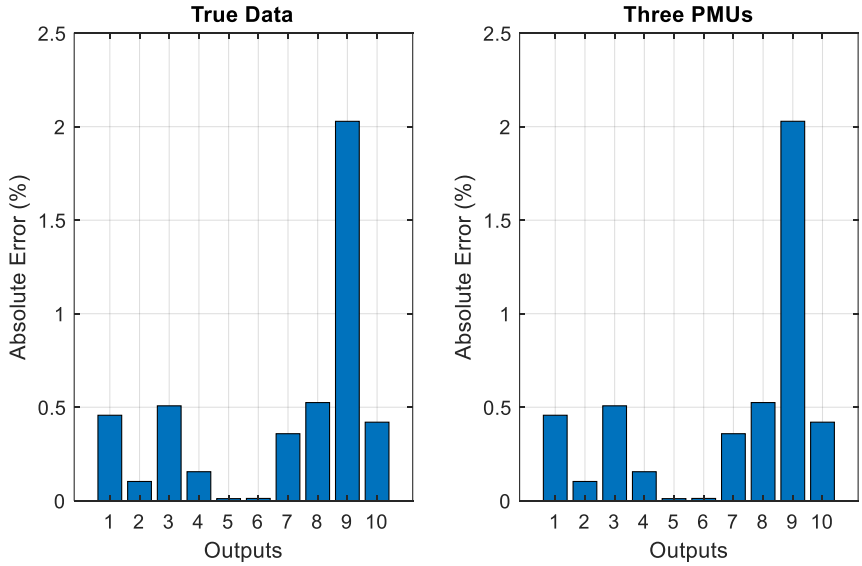

Figure 13. Prediction eigenvalues error for the third PMU location

4. CONCLUSION. In conclusion, the findings presented in this study underscore the significant potential of Artificial Neural Networks (ANN) in accurately predicting oscillation modes based on bus angle measurements obtained through Phasor Measurement Units (PMUs). The success of this prediction process is grounded in the utilization of ambient measurements, showcasing the applicability and effectiveness of data-driven methodologies in power grid stability assessment.

The results vividly demonstrate that the ANN model achieves commendable accuracy in forecasting oscillation modes, a critical facet of ensuring power system stability and resilience. This achievement is a testament to the intricate capabilities of the ANN model to harness the inherent patterns within the measured angles of buses, thereby providing a valuable tool for real-time decision-making and control in power systems.

Furthermore, this study introduces a novel approach to optimizing the sequence of PMU installations, leveraging the predictive power of the ANN-based oscillation mode prediction. By strategically placing PMUs based on the anticipated oscillation modes, system operators can enhance situational awareness and expedite response times, bolstering the overall stability and operational efficiency of the power grid.

As the energy landscape continues to evolve, the integration of advanced data-driven techniques like ANN promises to be instrumental in fortifying power system resilience and adaptability. This research contributes not only to the understanding of oscillation mode prediction but also offers practical insights into enhancing the deployment strategy of PMUs, thus heralding a new era of intelligent and predictive power grid management.

Acknowledgment. This work was supported by The Scientific Research and Innovation Support Fund (SRISF) / Jordan under project number (ENE/1/3/2020).

REFERENCES

[1] S. Okubo, H. Suzuki, and K. Uemura, ‘‘Modal analysis for power system dynamic stability,’’ IEEE Trans. Power App. Syst.*(through 1985), vol. PAS-97, no. 4, pp. 1313–1318, Jul. 1978.

[2] P. Ray, ‘‘Power system low frequency oscillation mode estimation using wide area measurement systems,’’ Eng. Sci. Technol., Int. J., vol. 20, no. 2, pp. 598–615, Apr. 2017.

[3] J. Sanchez-Gasca et al., ‘‘Identification of electromechanical modes in power system,’’ IEEE Task Force Rep., IEEE PES, Piscataway, NJ, USA, Tech. Rep. TP462, 2012. [Online]. Available: https://resourcecenter.ieeepes.org/publications/technical-reports/PESTR15.html

[4] K. S. Shim, H. K. Nam, and Y. C. Lim, ‘‘Use of Prony analysis to extract sync information of low frequency oscillation from measured data,’’ Eur. Trans. Electr. Power, vol. 21, no. 5, pp. 1746–1762, Jul. 2011.

[5] T. Sarkar and O. Pereira, ‘‘Using the matrix pencil method to estimate the parameters of a sum of complex exponentials,’’ IEEE Antennas Propag. Mag., vol. 37, no. 1, pp. 48–55, Feb. 1995.

[6] J. G. Philip and T. Jain, ‘‘Analysis of low frequency oscillations in power system using EMO ESPRIT,’’ Int. J. Electr. Power Energy Syst., vol. 95, pp. 499–506, Feb. 2018.

[7] C. Jakpattanajit, N. Hoonchareon, and A. Yokoyama, ‘‘On-line estimation of power system low frequency oscillatory modes in large power systems,’’ J. Int. Council Electr. Eng., vol. 1, no. 3, pp. 352–358, Jul. 2011.

[8] A. Almunif, L. Fan, and Z. Miao, ‘‘A tutorial on data-driven eigenvalue identification: Prony analysis, matrix pencil, and eigensystem realization algorithm,’’ Int. Trans. Electr. Energy Syst., vol. 30, no. 4, Apr. 2020, Art. no. e12283.

[9] J. R. Smith, F. Fatehi, C. S. Woods, J. F. Hauer, and D. J. Trudnowski, ‘‘Transfer function identification in power system applications,’’ IEEE Trans. Power Syst., vol.

8, no. 3, pp. 1282–1290, Aug. 1993.

[10] H. Khalilinia, L. Zhang, and V. Venkatasubramanian, ‘‘Fast frequencydomain decomposition for ambient oscillation monitoring,’’ IEEE Trans. Power Del., vol. 30, no. 3, pp. 1631–1633, Jun. 2015.

[11] T. Jiang, H. Yuan, H. Jia, N. Zhou, and F. Li, ‘‘Stochastic subspace identification-based approach for tracking inter-area oscillatory modes in bulk power system utilising synchrophasor measurements,’’ IET Gener., Transmiss. Distrib., vol. 9, no. 15, pp. 2409–2418, Nov. 2015.

[12] S. A. N. Sarmadi and V. Venkatasubramanian, ‘‘Electromechanical mode estimation using recursive adaptive stochastic subspace identification,’’ IEEE Trans. Power Syst., vol. 29, no. 1, pp. 349–358, Jan. 2014.

[13] L. Dosiek, N. Zhou, J. W. Pierre, Z. Huang, and D. J. Trudnowski, ‘‘Mode shape estimation algorithms under ambient conditions: A comparative review,’’ IEEE Trans. Power Syst., vol. 28, no. 2, pp. 779–787, May 2013.

[14] Al-Odienat, Abdullah, et al. "Low frequency oscillation analysis for dynamic performance of power systems." 2021 12th International Renewable Engineering Conference (IREC). IEEE, 2021.

[15] Gupta, Abhilash Kumar, Kusum Verma, and K. R. Niazi. "Wide-area PMU-ANN based monitoring of low frequency oscillations in a wind integrated power system." 2018 8th IEEE India International Conference on Power Electronics (IICPE). IEEE, 2018.

[16] Al-Odienat, A. I., et al. "Connectivity Matrix Algorithm: A New Optimal Phasor Measurement Unit Placement Algorithm." IOP Conference Series: Earth and Environmental Science. Vol. 551. No. 1. IOP Publishing, 2020